Int. J. Heat Mass Transfer. Vol. 11, pp. 1215–1224. Pergamon Press 1968. Printed in Great Britain

FREE CONVECTION ORGANIC SUBLIMATION ON A VERTICAL SEMI-INFINITE PLATE

JAMES A. ADAMS* and ROBERT L. LOWELL, Jr.†
Engineering Department, Unites States Naval Academy, Annapolis, Maryland, U.S.A.

(*Received* 23 *October* 1967 *and in revised form* 4 *March* 1968)

Abstract—The nonlinear, partial differential equations defining free convection boundary-layer flow along a vertical, flat, subliming, nonreacting surface were solved by means of a similarity transformation and a numerical method of asymptotic iteration through the boundary layer. The ambient temperature and pressure were varied to observe the resulting effect on the Nusselt and Sherwood numbers. Particular interest was directed to the effect of the pressure ratio (P_∞/P_{bw}) near regions of flow instability caused by the interaction of buoyancy and gravitational forces in the boundary layer. The results indicated that the ambient pressure can have a significant effect on convective heat and mass transfer in certain, well defined regions.

NOMENCLATURE

C, constant defined in equation (9);
D, mass diffusivity;
F', dimensionless velocity function;
g, gravitation acceleration;
h, convection coefficient;
k, thermal conductivity;
M, molecular weight;
P, pressure;
T, temperature;
u, v, flow velocity in the x and y directions respectively;
x, y, coordinate axes measured parallel and normal to the plate respectively;
X, body force defined in equation (7);
Gr_x, local Grashof number;
Nu_x, local Nusselt number;
Pr, Prandtl number;
Sc, Schmidt number;
Sh_x, local Sherwood number.

Greek symbols

α, thermal diffusivity;
δ, boundary-layer thickness;
η, similarity variable;
θ, dimensionless temperature function;
Λ, dimensionless body force, $= X/X_w$;
ν, kinematic viscosity;
ρ, density;
ϕ, dimensionless mass fraction ratio;
ψ, stream function;
ω, mass fraction.

Subscripts

a, free stream component;
b, subliming component;
w, wall condition;
∞, free stream condition.

INTRODUCTION

DURING recent years, the behavior of multi-component boundary layers has been the subject of considerable study, particularly with reference to mass injection through a porous wall. The standard heat-transfer problem for both forced and free convection was compounded by the additional mass transfer, resulting in increased interest in the coupling effects of thermal diffusion (Soret effect) and diffusion thermo (Dufour effect) for certain conditions. References [1, 2] contain bibliographies and discussion of this effort.

This paper is concerned with the boundary-

* Associate Professor, USNA.
† Ensign, U.S. Navy.

layer behavior on a vertical subliming organic surface in air and the instabilities that occur when the magnitude of the upward temperature induced buoyancy force is nearly equal to the magnitude of the downward gravitational attraction on the subliming component. For example, such a region of flow instability might occur during the sublimation of a heavy organic vapor from a heated surface. Such regions were noted in [1] with regard to heavy injected gases such as carbon dioxide, argon and xenon. Special emphasis in the present analysis is given to the effect of the ambient conditions of pressure and temperature on the behavior of the multicomponent boundary layer.

Numerical solutions to the governing differential equations were obtained for three different subliming materials. Para-dichlorobenzene (*p*-$C_6H_4Cl_2$) was chosen because experimental results were available for free convection sublimation into air at atmospheric pressure [11]. The other two organic materials, naphthalene ($C_{10}H_8$) and camphor ($C_{10}H_{16}O$), were chosen as being representative of commonly used organic materials.

A discussion of the theoretical model used in the analysis is given below along with important assumptions. The formulation of the body force in the momentum equation and the transformed set of equations used to obtain the final results are presented.

THEORETICAL MODEL

The basic equations which were analyzed are as follows:

continuity:

$$\frac{\partial u}{\partial x} + \frac{\partial v}{\partial y} = 0 \tag{1}$$

momentum:

$$u\frac{\partial u}{\partial x} + v\frac{\partial u}{\partial y} = \nu\frac{\partial^2 u}{\partial y^2} + g\left(\frac{\rho_\infty}{\rho} - 1\right) \tag{2}$$

energy:

$$u\frac{\partial T}{\partial x} + v\frac{\partial T}{\partial y} = \alpha\frac{\partial^2 T}{\partial y^2} \tag{3}$$

species:

$$u\frac{\partial \omega_b}{\partial x} + v\frac{\partial \omega_b}{\partial y} = D_{ab}\frac{\partial^2 \omega_b}{\partial y^2} \tag{4}$$

state:

$$\rho = \rho(\omega_b, T) \tag{5}$$

with the accompanying boundary conditions,

$$\left.\begin{aligned} &\text{at} \quad y = 0: \quad u = 0; \quad v = v_w; \\ &\qquad\qquad\quad T = T_w; \quad \omega = \omega_{bw} \\ &\text{at} \quad y \to \infty: \quad u = 0; \quad T = T_\infty; \\ &\qquad\qquad\quad \omega_b = \omega_{b\infty} = 0. \end{aligned}\right\} \tag{6}$$

The model used in this investigation was the steady-state, two-dimensional, laminar, free convection boundary layer with constant transport properties on a vertical, flat, nonreacting surface. Figure 1 shows a model sketch for $T_w > T_\infty$ with the boundary layers growing from the bottom of the plate. When $T_w < T_\infty$, the boundary layers were assumed to grow from the top of the plate. The simplifications inherent in the basic equations are discussed briefly in the following paragraphs.

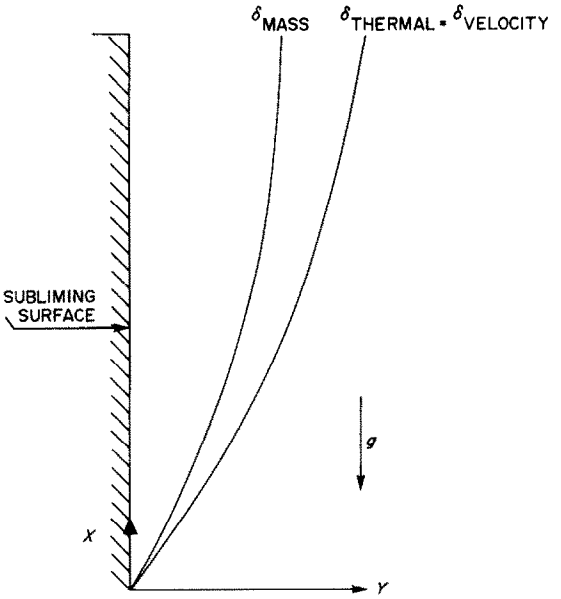

FIG. 1. Physical model for simultaneous heat and mass transfer from a subliming surface.

The Soret and Dufour effects mentioned earlier were negligible for this model since the investigation was concerned with heavy, organic materials, and consequently were omitted from the species and energy equations. Although Sparrow *et al.* [3] found that light gases such as helium could cause large diffusion thermo effects under certain conditions, a previous report [4] indicated that such effects were negligible for heavier gases such as CO_2, A and Xe.

A study of the effects of physical property variation on binary diffusion and heat transfer on a vertical surface reported by Gill *et al.* [5] has shown that for CO_2, the heaviest gas considered, close agreement was obtained in calculating the Nusselt number whether or not the physical parameters (except the density in the body force term of the momentum equation) were allowed to vary as a function of temperature and pressure. Such an approximation cannot be made for the lighter gases considered in [5], but was justified in this study due to the relatively large atomic masses of the organic materials used. Care should be taken, however, that the average values selected for these parameters are applicable for the specific temperatures and pressures used later in setting up corresponding temperature and pressure ratios.

In order to analytically define the problem, it was assumed that both the subliming organic vapor and the surrounding air behaved as perfect gases. From the boundary conditions, it may be noted that subliming material was assumed to be nonexistent in the free stream.

Experimental evidence has shown that flow instabilities on a vertical subliming surface are dominant for Grashof numbers less than 10^5. Thus, no meaningful results were anticipated outside the Grashof range between $10^5 < Gr < 10^9$. The effect of viscous dissipation was also neglected.

Since the density was a function of both temperature and mass fraction of the organic vapor, the momentum, energy, and species equations were coupled through the body force term in the momentum equation. By using the perfect gas relationships, assuming local thermodynamic equilibrium, and constant total pressure across the boundary layer, this term was expressed by the following:

$$X = g\left(\frac{\rho_\infty}{\rho} - 1\right)$$

$$= g\left\{\frac{T\left[1 + \left(\frac{M_b - M_a}{M_a}\right)\left(\frac{P_{b\infty}}{P}\right)\right]}{T_\infty\left[1 + \left(\frac{M_b - M_a}{M_a}\right)\left(\frac{P_b}{P}\right)\right]} - 1\right\}. \tag{7}$$

Finally, to express the body force in terms of the dependent variables T and ω_b, the above expression was rearranged to give,

$$X = g\left[\frac{1}{\frac{T_\infty}{T} + \left(1 - \frac{M_a}{M_b}\right)\omega_b} - 1\right] \tag{8}$$

where $P_{b\infty}$ was set equal to zero, by assuming pure air outside of the boundary layer, and

$$\omega_b = \frac{1}{\frac{M_a}{M_b}\left(\frac{P_\infty}{P} - 1\right) + 1}.$$

The total pressure P was practically equal to P_a due to the magnitude of the organic vapor pressures. When $M_a = M_b$, or $\omega_b = 0$, the body force term reduces to the usual form found in free convection heat-transfer problems.

The next step in the solution was to transform the nonlinear coupled set of partial differential equations to ordinary differential equations prior to a simultaneous solution. To effect this, a similarity analysis was applied. The defining equations (1–5) were expressed in terms of a single nondimensional, similarity variable $\eta = Cyx^{-\frac{1}{4}}$ and $\psi = 4Cvx^{\frac{3}{4}}F(\eta)$, where

$$C = \left\{\frac{g}{4\nu^2}\left[\frac{1}{\frac{T_\infty}{T_w} + \left(1 - \frac{M_a}{M_b}\right)\omega_{bw}} - 1\right]\right\}^{\frac{1}{4}} \tag{9}$$

and hence, were reduced from partial to ordinary differential equations as follows:

momentum:

$$F''' + 3FF'' - 2(F')^2 + \Lambda = 0 \quad (10)$$

energy:

$$\theta'' + 3PrF\theta' = 0 \quad (11)$$

species:

$$\phi'' + 3ScF\phi' = 0 \quad (12)$$

with transformed boundary conditions:

$$\left.\begin{aligned} &\text{at} \quad \eta = 0: \quad F(0) = \frac{\omega_{bw}}{1 - \omega_{bw}} \frac{\phi'(0)}{3Sc}; \\ &F'(0) = 0; \qquad \theta(0) = 1{\cdot}0; \\ &\phi(0) = 1{\cdot}0 \\ &\text{at} \quad \eta \to \infty: \quad \lim_{\eta \to \infty} F' = 0; \\ &\lim_{\eta \to \infty} \theta = 0; \qquad \lim_{\eta \to \infty} \phi = 0. \end{aligned}\right\} \quad (13)$$

The primes denote total differentiation with respect to the similarity variable η. Note that the nonlinearity has been retained through the transformation. The boundary condition relationship between $F(0)$ and $\phi'(0)$ was discussed by Eckert and Drake [6]. A derivation of the above similarity transformation by means of the group theory method of analysis can be found in [7], where it was pointed out that due to the complexity of the body force term, the only boundary condition permitting such an analysis was that of an isothermal surface.

The local convection coefficient was expressed by:

$$h = -\frac{k}{T_w - T_\infty}\left(\frac{\partial T}{\partial y}\right)_{y=0} = -Ckx^{-\frac{1}{4}}\theta'(0) \quad (14)$$

and the resulting local Nusselt number by,

$$Nu_x = \frac{hx}{k} = -Cx^{\frac{3}{4}}\theta'(0) = -\left(\frac{Gr_x}{4}\right)^{\frac{1}{4}}\theta'(0). \quad (15)$$

In a similar manner, the local Sherwood number was found to be,

$$Sh_x = -Cx^{\frac{3}{4}}\phi'(0) = -\left(\frac{Gr_x}{4}\right)^{\frac{1}{4}}\phi'(0). \quad (16)$$

From the above equations it can be seen that the definition of the local Grashof number is given by:

$$Gr_x = \frac{gx^3}{\nu^2}\left[\frac{1}{\frac{T_\infty}{T_w} + \left(1 - \frac{M_a}{M_b}\right)\omega_{bw}} - 1\right]. \quad (17)$$

The Nusselt and Sherwood numbers were determined by simultaneously solving the transformed ordinary differential equations (10–13) to find the nondimensional temperature and density gradients, $\theta'(0)$ and $\phi'(0)$ respectively. The technique used to obtain this solution is discussed in the next section.

Table 1 summarizes the numerical values of the physical properties used in the numerical calculations. All properties were assumed constant except the variation of organic vapor pressure (P_{bw}) with surface temperature (T_w), and the density variation in the body force term.

RESULTS

Numerical solutions to the transformed set of coupled, nonlinear, differential equations were obtained on an IBM 7030 computer, utilizing a modification of a program suggested by Nachtsheim and Swigert [8]. This program employed double precision and both the Runge–Kutta and Adams–Moulton integration schemes to provide asymptotic iteration throughout the boundary layer. By using an automatic initial-value routine, the missing boundary conditions of the nondimensional velocity, temperature; and organic mass gradients at the wall [$F''(0)$, $\theta'(0)$, $\phi'(0)$] were found. In this manner, solutions were obtained which satisfied the outer boundary conditions to the fourth decimal place. As anticipated, regions were encountered where no solutions could be obtained. These occurred when the opposing body force terms due to temperature and organic vapor concentration

Table 1. Physical properties

Material	Properties	Reference
p-dichlorobenzene	(a) $\log_{10} P_b$ (lb/ft^2) = 11·518–5946·0/T_w (°R)	[12]
(p-$C_6H_4Cl_2$)	(b) Sc = 2·23	[10]
	(c) M_b = 147·0	[13]
camphor	(a) $\log_{10} P_b$ (mm Hg) = 8·799–2797·4/T_w (°K)	[13]
($C_{10}H_{16}O$)	(b) Sc = 2·60	[10]
	(c) M_b = 152·2	[13]
naphthalene	(a) $\log_{10} P_b$ (mm Hg) = 11·450–3729·3/T_w (°K)	[13]
($C_{10}H_8$)	(b) Sc = 2·57	[10]
	(c) M_b = 128·1	[13]
air	(a) $\nu = 1{\cdot}8 \times 10^{-4}$ ft^2/s	[6]
	(b) Pr = 0·72	[6]
	(c) M_a = 28·96	[6]

differences were nearly equal. Physically these regions were associated with flow instabilities, where a similarity analysis of a laminar boundary layer would not be applicable.

The behavior of the body force for *p*-dichlorobenzene is shown in Fig. 2 in terms of the Grashof number expressed as a function of temperature and pressure ratios, T_w/T_∞ and P_∞/P_{bw} for x equal to unity. Other organics show a similar behavior. Solutions which were obtained near the region where the net body force changed directions were of greatest interest. The nondimensional temperature gradients at the wall obtained from the solution to the set of transformed equations are shown in Fig. 3. A similar behavior of the nondimensional organic mass gradients was obtained, as shown in Table 2.

The information from Figs. 2 and 3 was combined to form the Nusselt number according to equation (15). At a given temperature and pressure ratio, the Nusselt number was the product of $(Gr_x/4)^{\frac{1}{4}}$ given in Fig. 2 and $-\theta'(0)$ given in Fig. 3. The relationship between the Nusselt and Grashof numbers appears in Fig. 4. In each of the figures the effect of varying the pressure ratio P_∞/P_{bw} is evident.

CONCLUSIONS

It is instructive to compare the results in Fig. 3 with the calculations for free convection heat transfer reported by Ostrach [9]. For a Prandtl number of 0·72, a nondimensional wall temperature gradient of $-\theta'(0) = 0{\cdot}5046$ was obtained. The values of $-\theta'(0)$ reported in this study approached this value very closely in certain regions. For example, for a pressure ratio $P_\infty/P_{bw} = 1000$, the value for $-\theta'(0)$ agrees well with Ostrach's value outside the region $0{\cdot}94 < T_w/T_\infty < 1{\cdot}08$. It should be noted that at all pressure ratios greater than 500, very little deviation from the results for $P_\infty/P_{bw} = 1000$ occurred. For $P_\infty/P_{bw} = 100$, good agreement with Ostrach was obtained outside the region $0{\cdot}7 < T_w/T_\infty < 1{\cdot}5$. Thus, in certain regions the Nusselt number for a subliming surface can be found by using heat-transfer results, provided that the Grashof number is defined according to equation (17).

As the pressure ratio decreased, the regions where heat-transfer results were invalid became larger. Within these regions two separate observations were noted. First, a significant deviation in the values of $-\theta'(0)$ occurred, even though these values resulted from solutions conforming to the same convergence criteria as previous runs. Second, regions were encountered where boundary conditions could not be met, and hence, no results were obtained. The regions of no solution are obvious in Fig. 3. Such a region was very small for pressure ratios of $P_\infty/P_{bw} = 1000$ but as the ratio decreased, the region

Table 2. Tabulation of results

Material: P − $C_6H_4Cl_2$; Pressure ratio P_∞/P_{bw} = 1000				Material: ($C_{10}H_8$); Pressure ratio P_∞/P_{bw} = 100			
T_w/T_∞	$F''(0)$	$-\theta'(0)$	$-\phi'(0)$	T_w/T_∞	$F''(0)$	$-\theta'(0)$	$-\phi'(0)$
0·600	0·675824	0·503795	0·842487	0·600	0·674442	0·497913	0·873326
0·800	0·674948	0·503301	0·841836	0·781	0·668590	0·494634	0·688893
0·945	0·670806	0·501033	0·838812	0·820	0·665677	0·493028	0·866709
0·984	0·656161	0·492785	0·827895	0·950	0·634446	0·474828	0·842308
0·992	0·641839	0·484244	0·816777	0·991	0·581421	0·436567	0·794778
1·010	0·768253	0·547371	0·902787	1·056	0·881579	0·583244	0·998345
1·038	0·691094	0·511757	0·853259	1·085	0·770655	0·542022	0·936632
1·095	0·682223	0·507145	0·847020	1·140	0·729190	0·524143	0·910640
1·200	0·679752	0·505827	0·845251	1·267	0·708103	0·514263	0·896570
1·425	0·678739	0·505262	0·844506	1·425	0·701754	0·511086	0·892143
Material: P − $C_6H_4Cl_2$; Pressure ratio P_∞/P_{bw} = 845				Material: ($C_{10}H_{16}O$); Pressure ratio: P_∞/P_{bw} = 1000			
0·937	0·662498	0·498807	0·834869	0·600	0·675747	0·503793	0·897797
0·971	0·654665	0·495423	0·829162	0·800	0·674699	0·503223	0·897004
0·980	0·649310	0·492197	0·825017	9·945	0·669828	0·500634	0·893357
0·989	0·643836	0·485317	0·817912	0·984	0·652762	0·491261	0·880271
0·998	0·592630	0·451192	0·775180	0·992	0·636247	0·481599	0·867038
0·999	0·565073	0·423796	0·745317	1·010	0·788252	0·554484	0·972222
1·008	0·844605	0·581593	0·950355	1·038	0·693758	0·512894	0·910815
1·011	0·743652	0·540423	0·891514	1·095	0·683240	0·507606	0·903250
1·027	0·690875	0·515981	0·855997	1·200	0·680315	0·506096	0·901106
1·068	0·676100	0·508169	0·845665	1·425	0·679100	0·505444	0·900195
Material: P − $C_6H_4Cl_2$; Pressure ratio: P_∞/P_{bw} = 100				Material: ($C_{10}H_{16}O$); Pressure ratio: P_∞/P_{bw} = 100			
0·600	0·674793	0·496665	0·820665	0·600	0·674122	0·496684	0·873251
0·781	0·668868	0·493226	0·816265	0·781	0·667073	0·492730	0·867914
0·820	0·666035	0·491642	0·814291	0·820	0·663644	0·490822	0·865323
0·891	0·656359	0·485999	0·806971	0·950	0·628875	0·470230	0·837877
0·950	0·635726	0·473339	0·790974	0·991	0·577287	0·431802	0·790788
0·991	0·589716	0·439236	0·750660	1·056	1·079000	0·641025	1·08977
1·056	0·983485	0·615720	0·988478	1·086	0·814910	0·558224	0·962472
1·140	0·736755	0·526681	0·861306	1·140	0·747444	0·531025	0·922360
1·267	0·711854	0·514943	0·845377	1·268	0·717282	0·517403	0·902787
1·425	0·704721	0·511317	0·840568	1·425	0·708629	0·513190	0·896872

Table 2—continued

Material: P − $C_6H_4Cl_2$; Pressure ratio: P_∞/P_{hw} = 10				Material: ($C_{10}H_8$); Pressure ratio: P_∞/P_{hw} = 10			
0·600	0·671158	0·442162	0·650973	0·600	0·669197	0·450940	0·707979
0·877	0·639481	0·420655	0·629203	0·877	0·632530	0·426797	0·681955
0·966	0·615160	0·401126	0·610788	0·966	0·602877	0·403028	0·658397
0·991	0·605607	0·391957	0·602806	0·991	0·590746	0·390980	0·647588
1·530	1·46275	0·666802	0·933868	1·530	1·14784	0·610851	0·917045
1·541	1·27823	0·630017	0·885164	1·541	1·08146	0·594357	0·894379
1·583	1·17258	0·606504	0·854345	1·583	1·03538	0·582209	0·877822
1·629	1·10440	0·590096	0·833023	1·629	1·001765	0·572924	0·865256
1·730	1·02257	0·568778	0·805607	1·730	0·956730	0·559823	0·847687
1·900	0·960830	0·551179	0·783302	1·900	0·919134	0·548159	0·832260
Material: ($C_{10}H_8$); Pressure ratio: P_∞/P_{hw} = 1000				Material: ($C_{10}H_{16}O$); Pressure ratio: P_∞/P_{hw} = 10			
0·600	0·675789	0·503927	0·893968	0·600	0·668806	0·444024	0·686097
0·800	0·674951	0·503470	0·893334	0·877	0·632276	0·419460	0·660574
0·945	0·671012	0·501377	0·890396	0·966	0·605023	0·397071	0·639284
0·984	0·656737	0·493591	0·879538	0·991	0·594377	0·386332	0·630023
0·992	0·642176	0·485219	0·868044	1·530	1·75447	0·720248	1·05104
1·010	0·752466	0·539967	0·946219	1·541	1·45276	0·667904	0·978159
1·038	0·689814	0·511069	0·904130	1·583	1·29556	0·636552	0·934984
1·095	0·681719	0·506957	0·898282	1·629	1·19921	0·615431	0·906168
1·200	0·679422	0·505764	0·896597	1·730	1·08816	0·588739	0·870142
1·425	0·678464	0·505247	0·895878	1·900	1·00705	0·567141	0·841434

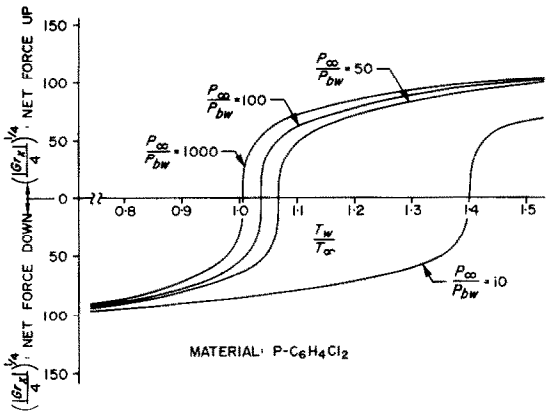

FIG. 2. Body force variation.

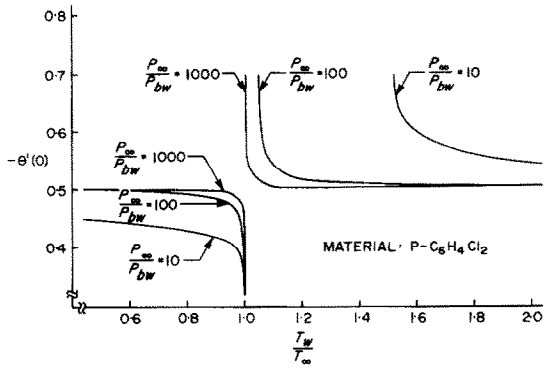

FIG. 3. Nondimensional temperature gradients.

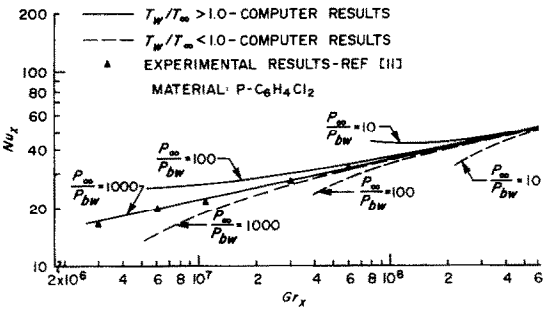

FIG. 4. Nusselt vs. Grashof.

became larger. For $P_\infty/P_{bw} = 100$, no solutions were obtained for $0{\cdot}998 < T_w/T_\infty < 1{\cdot}05$, and for $P_\infty/P_{bw} = 10$, no solutions were obtained for $0{\cdot}998 < T_w/T_\infty < 1{\cdot}52$. The valid solutions reported in this paper all occurred in the Grashof number range between 10^6 and 10^9.

Experimental measurements of heat-transfer rates from a subliming *p*-dichlorobenzene surface were reported in [11] for $T_w/T_\infty > 1{\cdot}0$ and pressure ranges between $200 < P_\infty/P_{bw} < 800$. The values so obtained, indicated in Fig. 4, agree well with the high pressure ratio results for $T_w/T_\infty > 1{\cdot}0$.

Two examples are given to indicate the heat-transfer effect predicted by these results. Consider free convection sublimation with $T_w/T_\infty = 1{\cdot}07$ and $P_\infty/P_{bw} = 845$. If the wall temperature is fixed and the environmental pressure is isothermally lowered until $P_\infty/P_{bw} = 100$, the value of $-\theta'(0)$ changes from 0·508 to 0·562, while that of $(Gr_x/4)^{\frac{1}{4}}$ changes from 67·0 to 52·4. Thus, the Nusselt number variation is from 34·1 to 29·4, a decrease of 13·8 per cent. On the other hand, if $T_w/T_\infty = 0{\cdot}95$ and the same pressure change occurs, the value of $-\theta'(0)$ changes from 0·496 to 0·473 while that of $(Gr_x/4)^{\frac{1}{4}}$ changes from 55·2 to 67·6. The resulting Nusselt number variation is from 27·3 to 32·0, an increase of 17·2 per cent. The same conclusions were reached by plotting the dimensional velocity profiles from the computer results. These plots clearly showed that a decrease in pressure ratio when $T_w/T_\infty > 1{\cdot}0$ produced a thicker boundary layer, whereas a decrease in pressure ratio when $T_w/T_\infty < 1{\cdot}0$ produced a thinner boundary layer. When the same pressure change occurred with T_w/T_∞ maintained at 1·5 or 0·6, there was very little change in the Nusselt number.

The mass-transfer behavior, as evidenced by variations in $\phi'(0)$ and the Sherwood number, followed a similar pattern. Graphs similar to Figs. 2 and 3 were obtained for heat and mass transfer for each of the organic materials studied. Tabulation of the data in Table 2 provides an accurate record of the results. The variation of $\theta'(0)$ and $\phi'(0)$ with pressure ratio, temperature ratio, and organic material can be seen in Table 2. For a given pressure, the variations became more pronounced as the region of instability was approached. Significant variations in both $\theta'(0)$ and $\phi'(0)$ also occurred for all temperature ratios as the pressure ratio

became smaller. For example, the difference between $\theta'(0)$ for camphor and naphthalene at $T_w/T_\infty = 0{\cdot}60$ was only 1·57 per cent at a pressure ratio of 10·0, but at the same pressure ratio, the difference between the $\theta'(0)$'s at $T_w/T_\infty = 1{\cdot}53$ was 15·2 per cent. At a pressure ratio of 1000, the difference between $\theta'(0)$ for camphor and naphthalene at $T_w/T_\infty = 1{\cdot}01$ was 2·6 per cent. The results clearly indicated the increasing effect of the mass transfer upon the heat transfer as the pressure ratio decreased, as well as the effect near the regions of instability.

ACKNOWLEDGEMENTS

The authors gratefully acknowledge the financial support of the Office of Naval Research through the United States Naval Academy Research Council, and the assistance received from personnel of the computer center at the U.S. Naval Weapons Laboratory, Dahlgren, Virginia.

REFERENCES

1. E. M. SPARROW, Recent studies relating to mass transfer cooling, *Proc. Heat Transf. Fluid Mech. Inst.*, 1–18 (1964).
2. D. W. ZEH and W. N. GILL, Binary diffusion and heat transfer in laminar boundary layers on vertical surfaces, A.I.Ch.E. Preprint 28 (1964).
3. E. M. SPARROW, W. J. MINKOWYCZ and E. R. G. ECKERT, Transpiration induced buoyancy and thermal diffusion–diffusion thermo in a helium–air free convection boundary layer. *J. Heat Transfer* **86**, 508–514 (1964).
4. E. M. SPARROW, W. J. MINKOWYCZ and E. R. G. ECKERT, Diffusion–thermo effects in stagnation point flow of air with injection of gases of various molecular weights into the boundary layer, *AIAA Jl* **2**, 654–659 (1964).
5. W. N. GILL, E. DEL CASAL and D. W. ZEH, Binary binary diffusion and heat transfer in laminar free convection boundary layers on a vertical surface, *Int. J. Heat Mass Transfer* **8**, 1135–1142 (1965).
6. E. R. G. ECKERT and R. M. DRAKE, *Heat and Mass Transfer*, pp. 460–462. McGraw-Hill, New York (1959).
7. R. L. LOWELL and J. A. ADAMS, Similarity analysis for multicomponent, free convection, *AIAA Jl* **5**, 1360–1362 (1967).
8. P. R. NACHTSHEIM and P. SWIGERT, Satisfaction of asymptotic boundary conditions in numerical solution of systems of nonlinear equations of the boundary-layer type, NASA TN D-3004 (1965).
9. S. OSTRACH, An analysis of laminar free convection flow and heat transfer about a flat plate parallel to the direction of the generating body force, NACA Report 1111 (1953).
10. C. H. BEDINGFIELD and T. B. DREW, Analogy between heat and mass transfer, *Ind. Engng Chem.* **42**, 1164–1173 (1950).
11. J. A. ADAMS and P. W. MCFADDEN, Simultaneous heat and mass transfer in free convection with opposing body forces, *A.I.Ch.E. Jl* **12**, 642–647 (1966).
12. H. H. SOGIN, Sublimation from disks to air streams flowing normal to their surfaces, *Trans. Am. Soc. Mech. Engrs* **80**, 61–67 (1958).
13. R. C. WEAST and S. M. SELBY (editors), *Handbook of Chemistry and Physics*, 47th edn, p. D-138. The Chemical Rubber Co., Cleveland, Ohio (1966).

Résumé—Les équations non-linéaires aux dérivées partielles définissant l'écoulement du type couche limite de convection naturelle le long d'une surface verticale plane sublimable et ne réagissant pas ont été résolues au moyen d'une transformation de similitude et d'une méthode numérique d'itération asymptotique à travers la couche limite. La température ambiante et la pression ont été modifiées pour observer l'effet résultant sur les nombres de Nusselt et de Sherwood. On s'est intéressé particulièrement à l'effet du rapport de pression (P_∞/P_{bw}) près des régions d'instabilité de l'écoulement provoqué par l'interaction des forces d'Archimède et de pesanteur dans la couche limite. Les résultats indiquaient que la pression ambiante pouvait avoir un effet sensible sur le transport de chaleur et de masse par convection dans certaines régions bien définies.

Zusammenfassung—Die nicht-linearen, partiellen Differentialgleichungen für die Grenzschichtströmung bei freier Konvektion an einer senkrechten, ebenen, sublimierenden, nicht-reagierenden Oberfläche wurden mit Hilfe einer Ähnlichkeits-Transformation und einer numerischen Methode der asymptotischen Iteration durch die Grenzschicht gelöst. Umgebungstemperatur und Druck wurden verändert, um die sich einstellenden Einflüsse auf die Nusselt- und Sherwood-Zahlen zu beobachten. Besonderes Interesse wurde den Einflüssen des Druckverhältnisses (P_∞/P_{bw}) geschenkt in der Nähe von strömungs-instabilen Bereichen, die auf der Wirkung von Auftriebs- und Schwerekräften in der Grenzschicht beruhen. Die Ergebnisse zeigen, dass der Umgebungsdruck einen deutlichen Einfluss auf den konvektiven Wärme- und Stoffübergang in gewissen, wohl definierten Bereichen haben kann.

Аннотация—С помощью автомодельных преобразований, а также метода асимптотической итерации по пограничному слою решены нелинейные дифференциальные уравнения в частных производных для пограничного слоя на вертикальной плоской сублимирующей нереагирующей поверхности при свободной конвекции. Исследовалось влияние окружающей температуры и давления на числа Нуссельта и Шервуда. Особое внимание обращалось на влияние отношений давления (P_∞/P_{bw}) вблизи областей неустойчивости, обусловленной взаимодействием подъемной и гравитационной сил в пограничном слое. Результаты показывают, что давление окружающей среды может оказывать сильное влияние на конвективный тепло-и массообмен в строго определенных областях.